

Green Synthesis, Characterization and Antibacterial Activity of Cobalt Nanoparticles from *Parkia biglobosa* Aqueous Stem Extract

Mela Yoro^{1*}, Japhet Joshua², Ayuba Isiyaku², Joyous Wilson Kitime Jonah², Patrick Datheh Bello²¹Department of Chemical Sciences, Faculty of Science, Federal University of Kashere, Gombe, Nigeria²Department of Science Laboratory Technology, Federal Polytechnic, Kaltungo, Gombe, NigeriaDOI: [10.36348/sijcms.2022.v05i05.003](https://doi.org/10.36348/sijcms.2022.v05i05.003)

| Received: 08.06.2022 | Accepted: 14.07.2022 | Published: 21.07.2022

*Corresponding author: Mela Yoro

Department of Chemical Sciences, Faculty of Science, Federal University of Kashere, Gombe, Nigeria

Abstract

In this research article, Cobalt nanoparticles were green synthesized, characterized and applied in antimicrobial study of some selected pathogens. The formation of cobalt nanoparticles was confirmed by first, its colour change from light brown to dark brown within 10 minutes. From the UV-Vis spectral analysis, it was observed that highest absorption peak appeared at 400nm reflecting the surface Plasmon resonance of Cobalt NPs from *Parkia biglobosa* stem which is characteristic of Cobalt Nanoparticles. From the FT-IR studies, the absorption peaks were seen at 3787.71 cm⁻¹, 3660.31 cm⁻¹, 3436.44 cm⁻¹, 1638.75 cm⁻¹, 1384.50 cm⁻¹, 1090.80 cm⁻¹ and 798 cm⁻¹. Investigation revealed a medium sharp peak absorption at 1090.80 cm⁻¹ which may be attributed to the stretching of aliphatic hydrocarbon (C-H). A peak at 1384.50 cm⁻¹ corresponds to C=C stretching while the absorption bands at 1638.75 cm⁻¹ and 3436.44 cm⁻¹ may be assigned to N-H and O-H stretching vibration modes respectively. Similarly, peaks were seen at 3787.71 cm⁻¹ and 3660.31 cm⁻¹ corresponding to O-H belonging to water and alcohol respectively. Furthermore, the very strong band at 798 cm⁻¹ emanates from C-O-C symmetric stretching and C-O-H bending vibrations of protein in the Cobalt nanoparticles. The surface morphology of the bio fabricated Cobalt nanoparticles, has revealed by SEM image, is spherical in shape having smooth surface and well dispersed with close compact arrangement. From the microbial study carried out, the surfaces of the cobalt nanoparticles might have interacted directly with the bacterial outer membrane, causing the membrane to rupture thereby killing the microbes. The antibacterial activity demonstrated by the cobalt nanoparticles in this study could be attributed to their small size and high surface to volume ratio, which therefore enables them to interact closely with bacterial membranes. From the minimum inhibitory concentration (MIC) study conducted, it showed clearly that the green synthesized cobalt nanoparticles inhibited the growth of the pathogens investigated.

Keywords: Green Synthesis, Characterization, Antibacterial Activity, Cobalt Nanoparticles, *Parkia biglobosa*, Aqueous Stem Extract.

Copyright © 2022 The Author(s): This is an open-access article distributed under the terms of the Creative Commons Attribution 4.0 International License (CC BY-NC 4.0) which permits unrestricted use, distribution, and reproduction in any medium for non-commercial use provided the original author and source are credited.

1. INTRODUCTION

Increasing awareness towards green chemistry and other biological processes has resulted to a desire to design an environmentally friendly approach for the synthesis of nanoparticles. Fabrication of metal, metal oxide or even their bimetallic nanoparticles using eco-friendly route without the use of toxic, harsh, and expensive chemicals remains the main principle of green chemistry and this method focuses on the usage of biocompatible reducing agents for synthesis of nanoparticles as reported in many literatures (Mela Y, *et al.*, 2022; Sharmila B.A, *et al.*, 2018; Bashpa P, *et al.*, 2017; Mahesh and Shivayogeeswar, 2018; Elisha K, *et al.*, 2020). Recently, many studies have proven that the

plant extracts act as a potential originator for the synthesis of the nanomaterials in harmless ways as they are used successfully in the synthesis of several greener nanoparticles. Nanoparticles display characteristic properties in their distribution, size and morphology. Furthermore, metallic nanoparticles have, over the years, become quite popular due to their unique properties and applications. Most transition metals including Silver, Cobalt, Iron, Copper, Gold, Platinum, Nickel among others, have been deployed in the synthesis of plants mediated nanoparticles (Flora P. J, *et al.*, 2018; Suriyavathana M, *et al.*, 2018; Mani P, *et al.*, 2016; Ravindra D.K, *et al.*, 2018; Shailesh C. K, *et al.*, 2018; Darshana R, *et al.*, 2020; Mela Y, *et al.*,

2022). In the same vein, Green synthesis of Cobalt nanoparticles, in particular, has gained momentum since the demand to synthesize nanoparticles in an eco-friendly way has increased significantly owing to their inherent characteristic of acting as an antimicrobial agent (Kuchekar S. R *et al.*, 2018). Significantly, it is worthy to note that, Nanoparticles are submicron moieties with diameters ranging from 1-100 nm made of inorganic or organic materials having novel properties as compared to the bulk materials (Mandep and Dimple, 2018). Nanotechnologies have gone way far by coupling two metals in a fascinating way to form bimetallic nanoparticles which are seen to have improved properties than their counter monometallic nanoparticles as reported by the previous studies (Wilson L.D, *et al.*, 2020; Mela Y *et al.*, 2022; Zaccheus S, *et al.*, 2020; Mela Y, *et al.*, 2022).



Figure 1: *Parkia biglobosa* plants

2.2.2 Preparation of aqueous plant extract

The collected stem barks were thoroughly washed under running tap water and rinsed severally with distilled water followed by sun-drying to remove residual moisture. The dried materials were cut into minute sizes and ground with the aid of a crucible. About 50 g of it was weighed and dispersed in 200 ml of sterile distilled water in a 500 ml glass beaker and boiled at 80°C for 20 min and were allowed to cool. After that, the solution was filtered through Whatman No.1 filter paper (Springfield Mill. Maid stone. Kent, England) and the filtrate was used immediately for the synthesis of cobalt nanoparticles.

2.2.3 Synthesis of Cobalt Nanoparticles

For the synthesis of cobalt nanoparticles, 10 ml of the aqueous leaf extract was added to 100 ml of 1×10^{-2} M aqueous $\text{Co}(\text{NO}_3)_2 \cdot 6\text{H}_2\text{O}$ solution in a 250 ml Erlenmeyer flask. Within 20min. change in colour was observed from light brown to dark brown indicating the formation of cobalt nanoparticles. The cobalt nanoparticles solution obtained was purified by

2. MATERIALS AND METHODS

2.1 Materials

The materials employed during this work include $\text{Co}(\text{NO}_3)_2 \cdot 6\text{H}_2\text{O}$ solution, *Parkia biglobosa* stem barks, deionized water, hot plate, Whatman no. 1 filter paper, crucible, beaker. All the reagents used during this work were of analytical grade.

2.2 Methods

2.2.1 Collection of plant materials

Fresh stem barks of *P. biglobosa* were collected from within the Garden located at Banganje, Billiri Local Government Area of Gombe State, Nigeria. The stem sample was transported via road to Federal University of Kashere, Gombe State, Nigeria. The same was identified and authenticated at the Taxonomy Section.

repeated centrifugation at 10,000 rpm for 15 min. followed by re-dispersion of the pellet in deionized water. Then the cobalt nanoparticles were dried in an oven at 80°C and then allowed to cool. The particles were stored in an airtight container

2.3 Characterization of the Co NPS

2.3.1 UV-visible Spectroscopy Analysis

The bio reduction process of cobalt ions in aqueous solution was measured by the sampling of 1 ml aliquot compared with 1 ml of distilled water used as blank and subsequently measuring the UV-visible spectrum of the solution. UV-visible spectrum was monitored on Cary Series UV-vis spectrophotometer Agilent Technology, operated within the wavelength range of 200 to 800 nm.

2.3.2 SEM Analysis

The surface morphology of the nanomaterial (CoNPs) was characterized by scanning electron microscope (SEM).

2.3.3. X-ray Diffraction (XRD) Analysis

The Size of the synthesized silver nanoparticles was investigated using X-ray diffractometer operating at a voltage of 45 kV and current of 40 mA with Cu K (α).

2.4. Antimicrobial analysis

Here, Agar well diffusion method was used for the antibacterial susceptibility assay. For this study, the test organisms were *Helicobacter pylori*, *Chlamydia trachomatis* (Gram-negative bacteria), *Staphylococcus aureus* and *Streptococcus pyogene* (Gram-Positive bacteria). The pure clinical isolates were obtained from the Pathology Laboratory of Gombe State University. All the clinical isolates were checked for purity and were maintained on nutrient broth at 4°C in the refrigerator for further use. Into sterile Petri dishes, nutrient agar was poured and allowed to solidify. On the solidified agar, 1ml of the test culture was dropped and the organism was spread all over the surface of the agar using a spreader. Using a sterile cork borer, wells of approximately 5 mm in diameter were made on the surface of the agar medium. The plates were turned upside down and the wells labelled with a marker. Each well was filled with 0.2 ml of the solution of cobalt nanoparticles. At 37°C, the plates were incubated aerobically for a period of 24 hours and the sensitivity of the organisms to the nanoparticles was noted. By comparing the different concentrations of the nanoparticles having different zones as well as selecting

the lowest concentration, the minimum inhibitory concentration (MIC) was determined.

3. RESULTS AND DISCUSSION

3.1 Cobalt Nanoparticles' Formation and UV-Visible Spectrophotometric Study

The formation of cobalt nanoparticles was initially monitored based on a change in colour of the reaction mixture at room temperature from light brown to dark brown within 10 min. after the nucleation of the metal ions indicating that phytoconstituents of *Parkia biglobosa* caused the reduction of Cobalt into CoNPs. This phenomenon might be attributed to the surface Plasmon absorption. Similarly, from the UV-Vis spectral analysis, it can be seen that highest absorption peak appeared at 400nm (Figure 2) reflecting the surface plasmon resonance of Cobalt NPs from *Parkia biglobosa* stem which is characteristic of Cobalt Nanoparticles. This finding is in concordance to the previous research reported by a separate researcher (Varaprasad T, *et al.*, 2017). Furthermore, the surface Plasmon absorption in the metal nanoparticles is due to the collective oscillation of the free conduction band electrons which is excited by the incident electromagnetic radiation. The colour change of the reaction mixture was also due to this surface Plasmon resonance phenomenon which provides a convenient indication of the formation of cobalt nanoparticles.

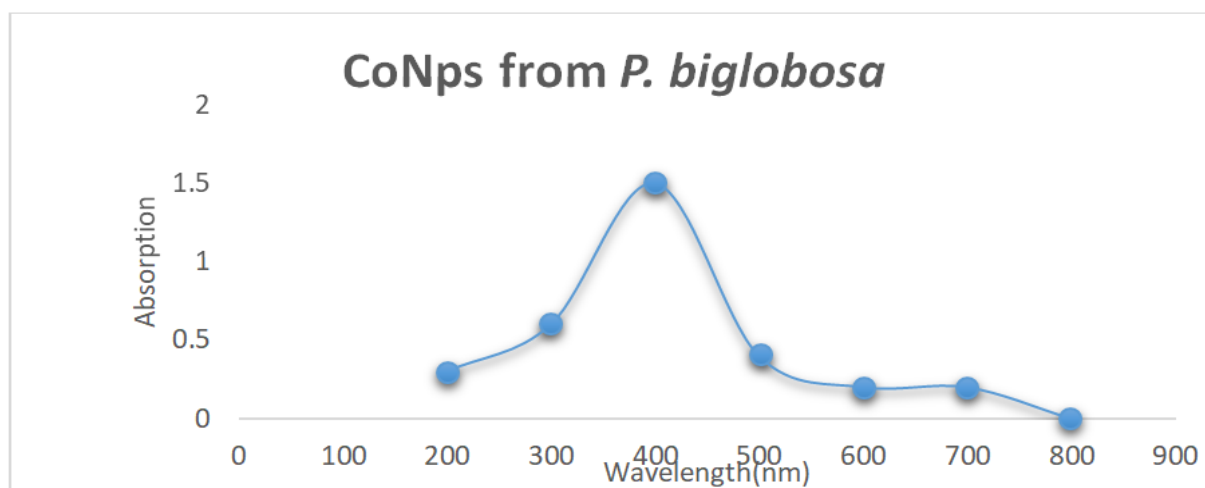


Figure 2: UV-visible Spectrum of Co NPs from *P. biglobosa* Stem Extract

3.2 FT-IR Analysis

FT-IR is employed to determine the different functional groups such as amine, alcohol, alkane,

alkynes, alkenes and other such groups present in the substance which here is Cobalt nano particles as shown in Figure 3.

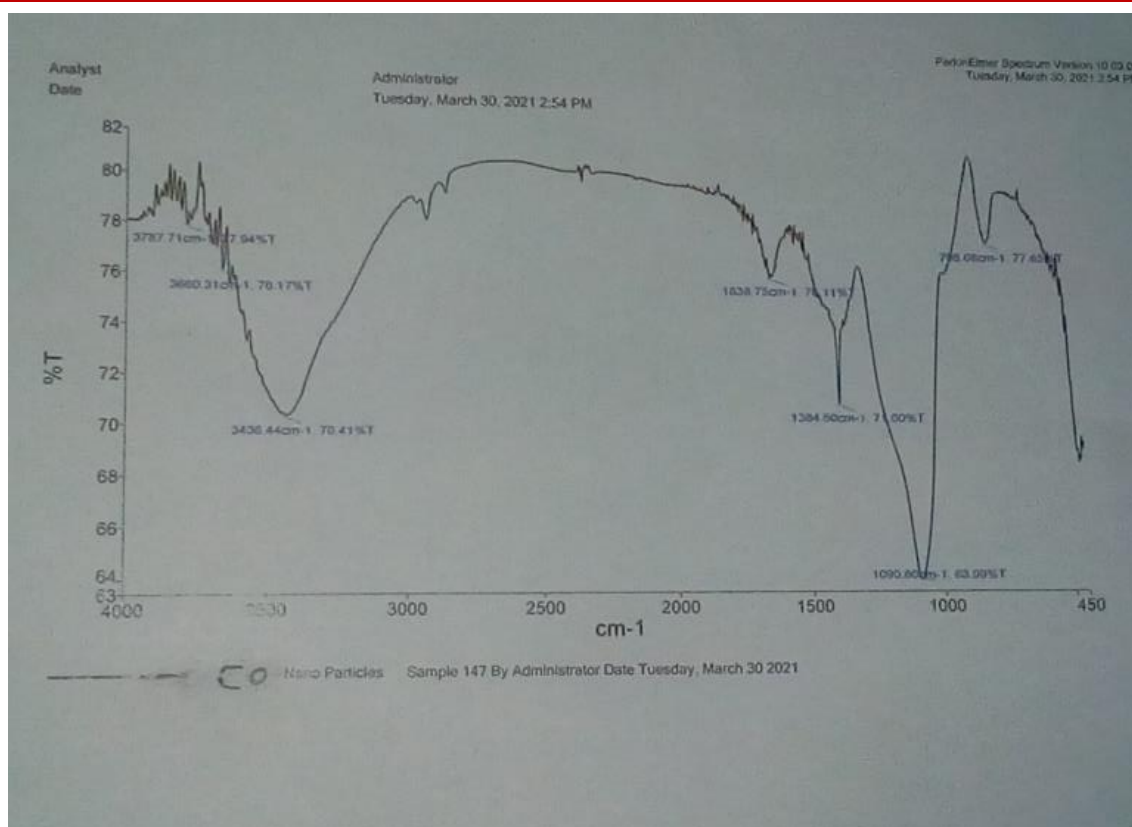


Figure 3: FT-IR spectrum of Cobalt nanoparticles from *P. biglobosa* Stem

The FTIR analysis was carried out to determine the number of phytoconstituents in stem bark extract of *P. biglobosa* plant acting as a stabilizing and capping agent in the presence of green synthesis. The

absorption peaks were studied from the above (Figure 3) FT-IR spectrum and the absorption bands summary was documented in table 1 below for easy interpretation.

Table 1: FT-IR studies of Cobalt nanoparticles

Peak(cm^{-1})	Functional group	V. Mode	Transmittance (%)	Intensity
3787.71	Water OH	Stretch	77.94	Weak
3660.31	Alcohol OH	Stretch	76.17	Weak
3436.44	OH	Stretch	70.41	Strong
1638.75	N-H	Stretch	76.11	Strong
1384.50	C=C	Stretch	71.00	Sharp
1090.80	C-H	Stretch	63.90	Sharp
798	C-O-C	Stretch	77.65	Weak

From the FT-IR studies (table 1), the absorption peaks were seen at 3787.71 cm^{-1} , 3660.31 cm^{-1} , 3436.44 cm^{-1} , 1638.75 cm^{-1} , 1384.50 cm^{-1} , 1090.80 cm^{-1} and 798 cm^{-1} . Investigation reveals a medium sharp peak absorption at 1090.80 cm^{-1} which may be attributed to the stretching of aliphatic hydrocarbon (C-H). A peak at 1384.50 cm^{-1} corresponds to C=C stretching while the absorption bands at 1638.75 cm^{-1} and 3436.44 cm^{-1} may be assigned to N-H and O-H stretching vibration modes respectively. Similarly, peaks were seen at 3787.71 cm^{-1} and 3660.31 cm^{-1} corresponding to O-H belonging to water and alcohol respectively. Furthermore, the very strong band at 798 cm^{-1} emanates from C-O-C symmetric stretching and C-O-H bending vibrations of protein in the Cobalt nanoparticles. The result of the FT-IR analysis

investigated in this study, is not only consistent with the UV-visible result, but also corresponds to the result of other researchers (Varaprasad T, *et al.*, 2017) which then confirmed the bio fabrication of Cobalt nanoparticles.

3.3 SEM Investigation

SEM image (figure 4) of Co NPs from *P. biglobosa* stem extract revealed that, it is spherical in shape having smooth surface and well dispersed with close compact arrangement. It is observed that the cobalt nanoparticles are scattered over the surface and no aggregates are noticed under SEM. More so, the Scherer rings characteristic of fcc Cobalt is apparently observed, showing that the structure seen in the SEM image are nano crystalline in nature. The biosynthesized Co NPs had been evenly distributed throughout the

solution. The findings of this study are consistent with prior research that found spherical Co NPs when synthesis was facilitated by plant extract (Varaprasad T,

et al., 2017; Igwe and Ekebo, 2018; Igwe and Mgbemene, 2014).

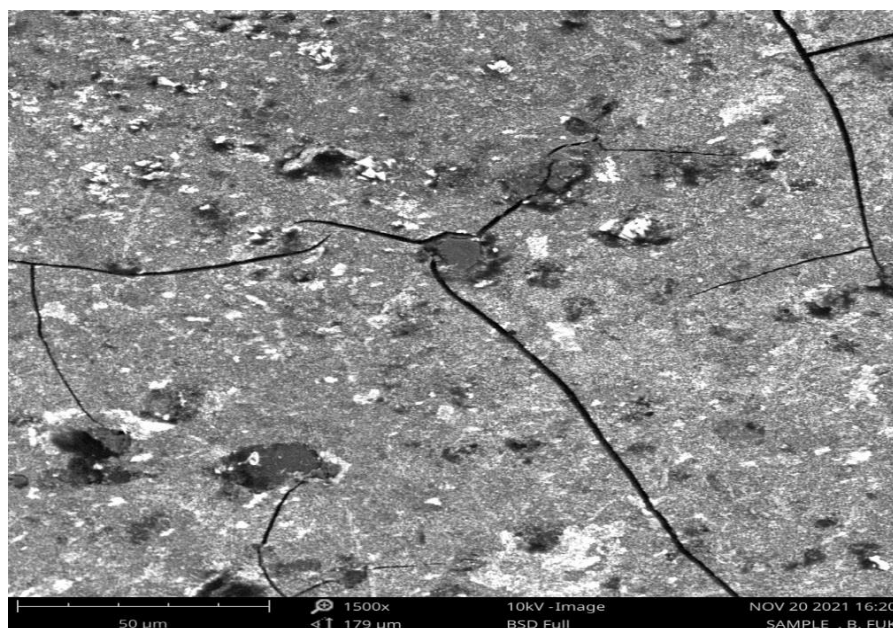


Figure 4: SEM Image of Cobalt Nanoparticles

3.4 Antibacterial susceptibility assay:

In this present research, flagyl was used as a positive control in the experiment and the zone of inhibition of cobalt nanoparticles green synthesized from the stem bark extract of *P. biglobosa* against four pathogenic microbes is shown in Table 2. Two each of Gram-negative and Gram-positive bacteria microbes were used for the study. These are human pathogens capable of causing diseases ranging from pneumonia, meningitis, skin infections, bacteraemia, sepsis, toxic shock syndrome, urinary tract infections, vomiting, anaemia, osteomyelitis, endocarditis, diarrhoea, lung infection, wound infections to kidney infections. The surfaces of the cobalt nanoparticles might have

interacted directly with the bacterial outer membrane, causing the membrane to rupture thereby killing the microbes. It therefore implies that, the antibacterial activity demonstrated by the cobalt nanoparticles in the current study is attributed to their small size and high surface to volume ratio, which therefore enables them to interact closely with bacterial membranes. The minimum inhibitory concentration (MIC) of the cobalt nanoparticles is shown in Table 3. Hence, it can be deduced that, the Cobalt nanoparticles synthesized inhibited the growth of the selected organisms, of course the result that is consistent the earlier literatures (Igwe and Ekebo, 2018; Igwe and Mgbemene, 2014)

Table 2: Zone of inhibition (mm) of cobalt nanoparticles against pathogens

Concentration of cobalt nanoparticles (mg/ml)	<i>H. pylori</i>	<i>C. trachomatis</i>	<i>S. aureus</i>	<i>S. pyogene</i>	Positive control (mm)
25.00	-	-	3.01	2.10	19.20
50.00	3.80	4.20	4.50	3.78	25.50
100.00	5.70	5.52	6.90	5.10	36.80

Table 3: Minimum inhibitory concentration of cobalt nanoparticles against pathogens

Concentration of cobalt nanoparticles (mg/ml)	<i>H. pylori</i>	<i>C. trachomatis</i>	<i>S. aureus</i>	<i>S. pyogene</i>	Positive control (Flagyl)
4.5	-	-	-	-	+
8.25	-	-	-	-	+
16.5	-	-	+	+	+
33.0	+	+	+	+	+

From the MIC, the degree of inhibition is summarized as
 $S. aureus = S. pyogene > H. pylori = C. trachomatis.$

4. CONCLUSION

The study examined the antimicrobial potency of Cobalt nanoparticles synthesized using green approach. The formation of cobalt nanoparticles was initially monitored based on colour change of the reaction mixture at room temperature from light brown to dark brown within a space of 10 min. UV analysis of the sample revealed that the maximum absorption peak was at absorbance of 1.5 with corresponding wavelength (λ max) at 400 nm. The sample was subjected to FT-IR and SEM analysis to determine the functional group and the surface morphology. Antibacterial study conducted revealed that cobalt nanoparticles inhibited the growth of *H. pylori*, *C. trachomatis*, *S. aureus* and *S. pyogene* thereby rendering it a potential antibacterial agent.

Authors' Contributions: This work was carried out in collaboration among all authors. Author MY designed the study, performed the statistical analysis, wrote the protocol and wrote the first draft of the manuscript. Authors JJ and AI managed the analyses of the study. Authors JWKJ and PDB managed literature searches. All authors read and approved the final manuscript.

Funding: This research received no external funding.

Acknowledgments: Authors wish to thank Federal University of Kashere for the work space.

Conflict of Interest: The authors declare that there is no conflict of interests regarding the publication of this manuscript.

REFERENCE

- Mela, Y., Amos, G., Japhet, J., & Ayuba, I. (2022). Green Synthesis, Characterization and Antimicrobial Potency of Silver Nanoparticles from *Psidium guajava* Leaf Extract. *Online Journal of Chemistry*, 2022(2), 14-22.
- Sharmila, B. A., Thirumurugan, V., & Amudha, M. (2018). Green Biosynthesis of Silver Nano Particles from *Aegle Marmelos* Aqueous Leaf Extract. *IOSR Journal of Applied Chemistry*, 11(7), 6-11.
- Bashpa, P., Seema, D. R., & Bijudas, K. (2017). Green synthesis of silver nanoparticles from *Orthosiphon thymiflorus* leaf extract. *International Journal of Green and Herbal Chemistry*, 6(4), 7-211.
- Mahesh, M. C., & Shivayogeeswar, E. N. (2018). Effect of Sheep and Goat Fecal Mediated Synthesis and Characterization of Silver Nanoparticles (AgNPs) and Their Antibacterial Effects. *Journal of Nanofluids*, 7(2018), 1-7.
- Elisha, K., Buhari, M., Zaccheus, S., & Hadiza, A. (2020). Green Synthesis of Silver Nanoparticles from *Solenostemon Monostachyus* Leaf Extract and In Vitro Antibacterial and Antifungal Evaluation. *European Journal of Advanced Chemistry Research*, 1(4), 1-5.
- Flora, P. J., Sivakumari, K., Rajini, S., Ashok, K., Jayaprakash, P., & Rajesh, S. (2018). Green Synthesis of Silver Nanoparticles from Propolis. *RJLBPCS*, 4(4), 23-36.
- Suriyavathana, M., Janeesha, K. J., Manikandan, M., Sandhya, M., & Ashok, R. K. (2018). Synthesis of Iron Nanoparticles (Fenp's) and Characterization of *Macrotyloma Uniflorum* Seed Extract. *International Journal of Green and Herbal Chemistry*, 7(3), 513-519.
- Mani, P., Vijay, R., Pragnesh, D., & Ekta, K. (2016). Phytochemical Screening and green Synthesis of Biogenic Silver Nanoparticle from Leaf Extract of *Pongamia Pinnata (L) Pierre* of Semi-Arid Region of Kachchh. *International Journal of Green and Herbal Chemistry*, 5(2), 172-181.
- Ravindra, D. K., Sangeeta, B., Prerana, K., & Sandeep, M. (2018). Synthesis and characterization of magnetite nanoparticles using betel leaves. *International Journal of Green and Herbal Chemistry*, 7(1), 43-152.
- Shailesh, C. K., Kokila, A. P., & Tessa, J. (2018). Green Synthesis of Silver Nanoparticles using *Elytraria acaulis* Plant Root Extract and its Antimicrobial activity. *International Journal of Green and Herbal Chemistry*, 7(3), 598-609.
- Darshana, R., Samrat, P., & Annika, D. G. (2020). Green Synthesis of Silver Nanoparticles Using Waste Tea Leaves. *Advanced Nano Research*, 3(1), 1-14
- Mela, Y., Ayuba, I., & Japhet, J. (2022). Evaluation of Antibacterial Efficacy of Green Synthesized Silver Nanoparticles from *Moringa Oliefera* Aqueous Root Extract. *International Journal of Advanced Multidisciplinary Research and Studies*, 2(3), 61-66.
- Kuchekar, S. R., Dhage, P. M., Aher, H. R., Han, S. H. (2018). Green synthesis of cobalt nanoparticles, its characterization and antimicrobial activities. *International Journal of Chemical and Physical Sciences*, 190-198.
- Mandeep, K., & Dimple, S. C. (2018). Green Synthesis of Iron Nanoparticles for Biomedical Applications. *Global Journal of Nano medicine*, 4(4), 1-10.
- Wilson, L. D., Zaccheus, S., Mela, Y., & Muhammad, M. A. (2020). Nanolarvicidal Effect of Green Synthesized Ag-Co Bimetallic Nanoparticles on *Culex quinquefasciatus* Mosquito. *Advances in Biological Chemistry*, 10, 16-23.
- Mela, Y., Japhet, J., & Isiyaku, A. (2022). Green Synthesis, Characterization and Antimicrobial Potency of Ag-Fe Bimetallic Nanoparticles from Papaya. *International Journal of Scientific and Research Publications*, 12(2), 563-568.

- Zaccheus, S., Wilson, L. D., Buhari, M., Muhammad, M. A., Musa, A. M., Abigail, J. M., & Yoro, M. (2020). Green Synthesis and Nanotoxicity Assay of Copper- Cobalt Bimetallic Nanoparticles as A Novel Nanolarvicide for Mosquito Larvae Management, *The International Journal of Biotechnology*, 9(2), 99-104.
- Mela, Y., Japhet, J., Ayuba, I., Joyous, W.K. J., & Patrick, D. B. (2022). Green Synthesis, Characterization and Antimicrobial Studies of Ag/Ni Bimetallic Nanoparticles from *Tamarindus indica* Aqueous Stem Extract. *International Journal of Advanced Multidisciplinary Research and Studies*, 2(3), 623-626.
- Varaprasad, T., Boddeti, G., & Venkateswara, R. B. (2017). Green Synthesized Cobalt Nanoparticles using *Asparagus racemosus* root Extract & Evaluation of Antibacterial activity. *International Journal of ChemTech Research* 10(9), 339-345.
- Igwe, O. U., & Ekebo, E. S. (2018). Biofabrication of cobalt Nanoparticles using leaf extract of *Chromolaena odorata* and their potential antibacterial application, *Research Journal of Chemical Sciences*, 8(1), 11-17.
- Igwe, O. U., & Mgbemene, N. M. (2014). Chemical investigation and antibacterial activity of the leaves of *Peperomia pellucid* L. HBK (Piperaceae). *Asian J Chem Pharm Res*, 2(1), 78-86.